High frequency oscillation in photonic crystal nanolasers

Tomoyuki Yoshie, Marko Lončar, Axel Scherer, and Yueming Qiu

Citation: Applied Physics Letters **84**, 3543 (2004); doi: 10.1063/1.1713051
View online: http://dx.doi.org/10.1063/1.1713051
View Table of Contents: http://scitation.aip.org/content/aip/journal/apl/84/18?ver=pdfcov
Published by the AIP Publishing

High frequency oscillation in photonic crystal nanolasers

Tomoyuki Yoshie,[a] Marko Lončar, and Axel Scherer
Department of Electrical Engineering, California Institute of Technology, Pasadena, California 91125-9300

Yueming Qiu
Jet Propulsion Laboratory, California Institute of Technology, Pasadena, California 91109

(Received 20 November 2003; accepted 26 February 2004; published online 20 April 2004)

We observed modulated oscillations in lasers of up to 130 GHz by conducting frequency domain measurements on photonic crystal lasers with built-in saturable absorbers. This is an example of how the small volumes of photonic crystal lasers lead to increases in the internal modulation frequencies and enables dramatic improvements of the laser modulation rate. © *2004 American Institute of Physics.* [DOI: 10.1063/1.1713051]

Optical nanocavities offer the unique ability to enhance or inhibit spontaneous emission,[1–4] and to generate high electric field. We have explored the fundamental limits of miniaturization of such optical cavities for photon localization, and have found that many of the functional building blocks for integrated optical systems, such as lasers, optical traps,[5] and logic gates greatly benefit from such miniaturization. Since photon localization[6,7] has been predicted to occur when introducing disorder within microfabricated photonic crystals,[8–10] much attention has been focused on finding the smallest localized mode with the smallest energy damping[11–13] in microfabricated photonic band-gap structures. One of the first devices based on localization of light in optical nanocavities was the photonic crystal laser,[14] described by several groups.[15–21] Here we show modulated oscillations in such lasers of up to 130 GHz from our frequency domain measurements.

Several designs of square and triangular lattice photonic crystals (PCs) were evaluated. Here we focus on the high-quality factor (Q) whispering gallery modes supported by square lattice photonic crystals.[12,16] Geometries of single-, double-, and quadruple-defect coupled cavities are shown in Fig. 1(a). The defect(s) were fabricated in the center of 21 by 21 square lattices of holes. We modeled the 2D photonic crystal slab cavity by using three-dimensional finite difference time domain (3D-FDTD) simulation, and calculated mode volumes (V_{mode}) of $0.6\times$, $0.8\times$, and $1.1\times(\lambda/n)^3$, and for cavities consisting of single-, two-, and four-coupled defects. To construct our lasers, four InGaAsP quantum wells were grown to form a 330 nm thick light-emitting slab on an InP substrate. A detailed method of fabricating our two-dimensional PC nanolasers is found in Ref. 17. In typical PC lasers, the lattice spacing (a) is 450 nm, and the slab thickness (d) is 330 nm. The porosity defined by r/a was varied between 0.34 and 0.36 and d/a was varied from 0.6 to 0.8. Calculated Q values ranged from 50 000 to 100 000 and λ, the resonance wavelength, was matched to the quantum well (QW) emission wavelength at 1550 nm. Experimental $\lambda/\Delta\lambda$ values range from 1000 to 6000 around the threshold. Figures 1(b) and 1(c) show typical amplitude profiles of the electric field obtained from a whispering gallery mode.

We tested all of our lasers by optically pumping them with an 830 nm laser diode at room temperature. The pump beam was focused to a 2 μm diameter spot and carefully aligned onto the center of our photonic crystal cavities. Part of emission from the PC nanolasers was directed through a $100\times$ objective lens and coupled into an optical fiber connected to an optical spectrum analyzer. The wavelength resolution of the analyzer was 0.2 nm, whereas the 2 μm optical pump beam was larger than the mode volume defined by $V_{\mathrm{mode}}=\int \epsilon(r)E^2(r)dV/\max[\epsilon(r)E^2(r)]$, and rendered most of the photonic crystal within that lasing mode transparent. However, the tails of the electric field from the lasing mode extend beyond the optically pumped transparent photonic crystal, and interact with unpumped absorbing material. The unpumped material surrounding the laser cavities functions as a passive saturable absorber that can give rise to nonlinear effects in photonic crystal nanolasers, such as bistability,[22] self-pulsation, and Q switching.

We have measured luminescence spectra as a function of peak pump power, and these are presented in Figs. 2(a) and 2(b) for 15 and 50 ns pulses separated by 50 μs on a quadruple-defect coupled cavity. Peak power is defined as

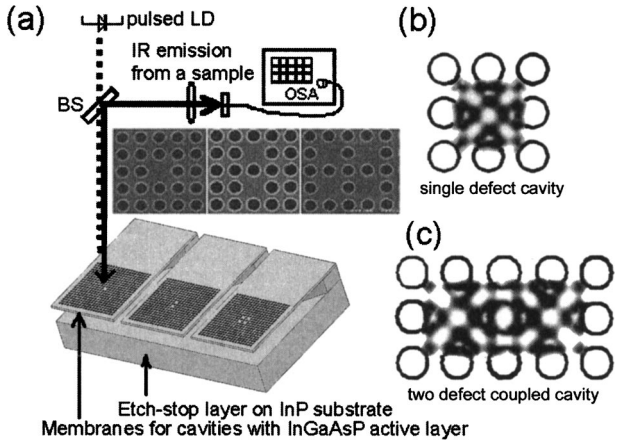

FIG. 1. Two-dimensional photonic crystal slabs with square lattice used in the work: (a) shows drawings of single defect, two-coupled defect, and four-coupled defect cavity membrane structures; (b) and (c) show electric field amplitude profiles in a middle of membrane for single defect and two-coupled defect cavity membrane structures, respectively. One of supermodes is shown for the two-defect coupled cavity.

[a]Electronic mail: yoshie@caltech.edu

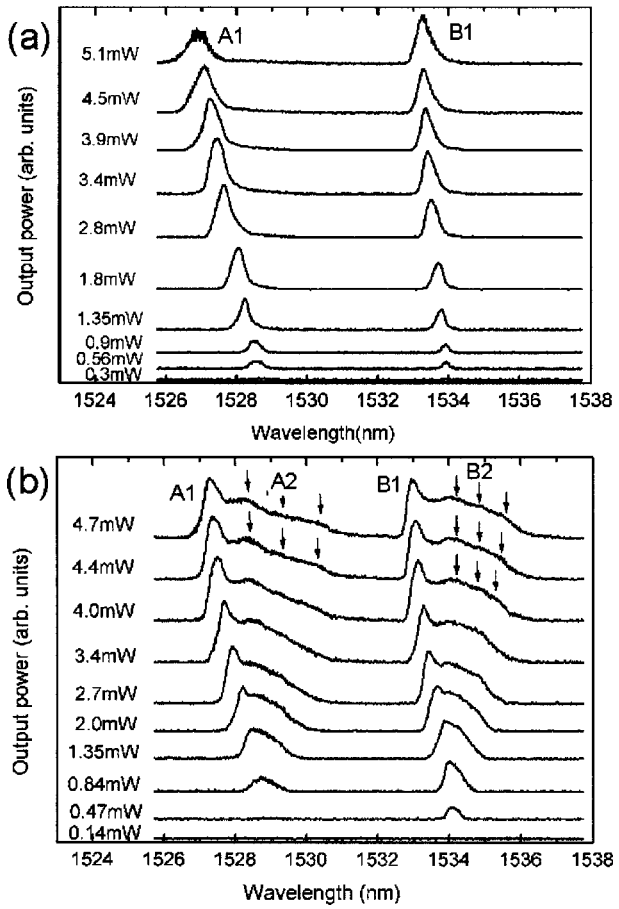

FIG. 2. Laser characteristics: (a) and (b) show luminescence spectra as a function of pumping peak power for 15 and 50 ns pulse operations, respectively, in four-defect coupled cavities. Peaks A2 and B2 are three equidistance peaks (one center peak and sidebands) after subtracting A1 and B1 with tails. The peak threshold pump powers are 200 μW for A1 and B1 peaks for 15 ns pulses. Sideband features are not seen at even higher pumping level for 15 ns pulse pumping. The blueshift of the sharp peaks (A1 and B1) might be caused by frequency pulling or denser electron-hole plasma effect.

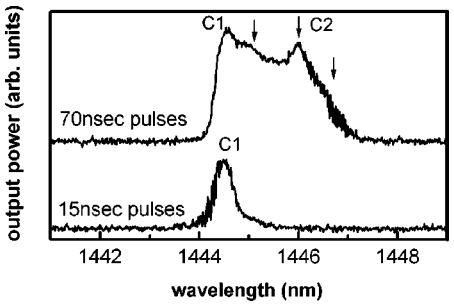

FIG. 3. Luminescence spectra measured by 15 and 70 ns pumping pulses with a 50 μs repeat rate at 77 K from a single defect square lattice photonic crystal slab cavity ($a=450$ nm, $r=0.34a$). The PC cavity supported single mode lasing of whispering gallery mode in this case. A center peak of C2 peaks are more pronounced than one in 50 ns pulses.

average power divided by the duty cycle. Comparisons with identical peak power pumping are appropriate to see changes of lasing spectra measured by different pulses. Two supermodes were pumped beyond the lasing threshold. The duty cycles for the pump beam under these conditions are 0.03% and 0.1%, respectively, limited to avoid cavity heating. At duty cycles below 1%, the luminescence spectra from our lasers are observed to broaden with increasing pump pulse length, and several smaller peaks emerge in the lasing spectrum. These additional peaks are not artifacts from cavity heating, but result from the time-resolved dynamics within nanolaser cavities that are surrounded by saturable absorbing QW material. Whereas clear symmetric peaks are apparent in measurements using 15 ns pulses, additional equidistant peaks (labeled A2 and B2), as well as extending tails of peaks A1 and B1 appear in 50 ns pulse measurements. Similar observations were made for all of our laser cavities, independent of the number of lasing modes. This pulse-length dependent spectral behavior even occurs in our triangular lattice photonic crystal lasers with fundamentally different cavity designs.[17] Separations of equidistant peaks depend upon modes as you can see from peaks A2 and B2.

We have made the following observations in this experiment: (1) A state with equidistance peaks is delayed to occur and the sharp peaks A1 and B1 initiate the occurrences of A2 and B2 peaks (switching from states 1 to states 2). (2) As the pump power is increased, three equidistance peaks are more pronounced and the spectral shifts are increased. Experimentally, we have confirmed that the QW saturable absorber surrounding the laser cavity provides the driving force, which gives rise to the additional spectral peaks, since the three equidistance peaks vanish when the pumping diameter is widened to cover the entire lasing mode. Moreover, the equidistant peaks are still observed at 77 K, only for longer pulses as shown in Fig. 3, which confirms that the sideband features do not result from sample heating, but from saturable absorption. This effect is not observed in quantum dot PC lasers,[16] possibly since the quantum dots do not provide enough absorption for nonlinear cavity behavior.

The three equidistance peaks, cannot be explained by mode locking. In mode locking, the spectral separation should be independent of the pumping conditions and instead would be dependent on the roundtrip of the cavity. The pumping pulses are rectangle shaped, and the Fourier-transformed signals theoretically have higher-order components. However, their effects are confirmed to be negligible by a spectrum analyzer. Instead, amplitude- or frequency-modulated oscillation, which depends on the pumping conditions of the laser cavity, explains our observation that these peaks remain at approximately the same relative spectral separation. Relaxation oscillation[23] or absorption-induced self-pulsation can be used to understand the amplitude-modulated oscillations. The relaxation frequency is given as a pole of the frequency response function of output power. When a cavity damping rate is faster than photon lifetime, the frequency is defined by

$$f_R=\frac{1}{2\pi}\sqrt{\frac{Sg_0}{\tau_p}}, \tag{1}$$

where S, g_0, and τ_p are photon density, temporal rate constant and photon lifetime, and f_R is an internal frequency defining the modulation speed of a laser. It should be noted that the absorption-induced self-pulsation frequency is smaller than the relaxation oscillation and that the frequency dependence on photon density is sometimes similar to the dependence of relaxation oscillation.[24] In order to extract the relation of frequencies and photon density, we deconvolved the spectrum into one sharp Lorentzian peak with a tail in

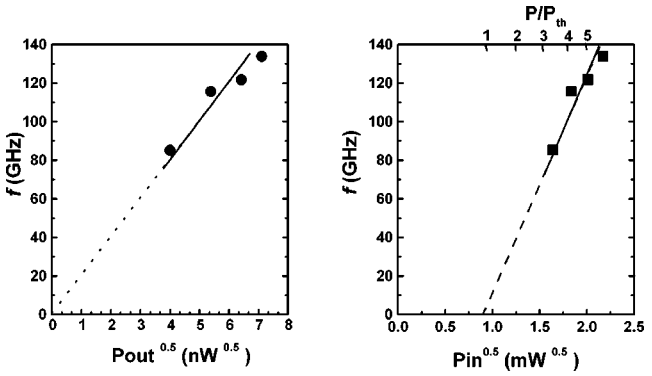

FIG. 4. (a) Shows frequency f as a function of square root of collected output peak power ($\sqrt{P_{\text{out}}}$). The sample was chosen such that the sample had the widest spacing between three equidistance peaks on pumping 50 ns pulsed with a period of 50 μs; (b) shows frequency f as a function of square root of collected input peak power ($\sqrt{P_{\text{in}}}$) to display pumping level. Data in (a) are used for (b). Small pumping level ($P/P_{th}<3$) did not exhibit clear sideband features. These observations match with our microcavity analysis results that relaxation oscillation peaks are seen for $P/P_{th}>3$.

longer wavelength and three equidistant subpeaks. The subpeak wavelengths and the integrated peak powers underneath each of these peaks were determined, and the sum of integrated peak power in all but the shortest wavelength peak was defined as $P_{\text{out}}(\propto S)$. Figures 4(a) and 4(b) show plots of frequency f, measured from the spacing between the equidistance peaks, as a function of (a) $\sqrt{P_{\text{out}}}$ and (b) $\sqrt{P_{\text{in}}}$ (square root of input peak power), respectively. The laser used for Fig. 4 was chosen to exhibit the maximum wavelength difference between the subpeaks, and was a two-defect coupled cavity ($a=460$ nm, $r=0.34a$) with a mode volume of $0.8(\lambda/n)^3$. The measured frequency is found to be proportional to the square root of output peak power as predicted from Eq. (1). The maximum measured frequency was $130(\pm 15)$ GHz, and could be tuned between $60(\pm 6)$ and $130(\pm 15)$ GHz by changing the precise cavity geometry and pumping condition. Most of nanolasers exhibit maximum frequencies of 60–100 GHz in our measurement range. The measured frequencies are consistent with microcavity laser theory.[25] The cutoff frequency resulting from cavity damping is 200 GHz at the wavelength for $Q=1000$. We show that a radical decrease in the mode volumes reducing photon lifetimes and increasing photon density enables an increase in modulation frequencies. The internal speed is determined by a slower rate of either damping rate or photon lifetime. A combination of small mode volume and moderate quality factor is key to make high-speed photonic crystal lasers whereas strong light-matter coupling requires high Q factors as well as small mode volumes. Due to the smaller photon number and the larger spontaneous emission coupling factor, the linewidth gets wider to obtain similar modulation frequency than one for conventional lasers. Whereas conventional lasers require 100 mW input power for 30 GHz operation,[26] the 130 GHz operation observed in PC lasers could be observed at surprisingly small absorbed power (of less than 1 mW). To construct practical high speed lasers, we need electrically pumped lasers and careful designs to avoid large RC components. By modification of the focused spot size of our optical pump beam, we can control the influence of the QWs surrounding the cavity. Although such tuning of the saturable absorber can be used to switch on the high frequency oscillations, we have not yet confirmed that our PC nanolasers are self-oscillating lasers or relaxation-oscillated lasers. Understanding the noise and the interplay between photons and carriers in the cavity and the absorber is essential to know the physics of the oscillations including the oscillation delay.

In summary, we have fabricated and tested high-Q planar photonic crystal cavities with mode volumes ranging between 0.6 and 1.2 cubic wavelengths and observed modulated oscillations up to 130 GHz. We reported the dynamic behavior of photonic crystal nanolasers by using the built-in saturable absorber.

The authors wish to acknowledge generous supports from the AFOSR and the DARPA. One of the authors (Y.Q.) would like to acknowledge the support from the Bio-Nano Program at the JPL, Caltech, under a contract with NASA.

[1] E. M. Purcell, Phys. Rev. **69**, 681 (1946).
[2] H. Yokoyama and S. D. Brorson, J. Appl. Phys. **66**, 4801 (1989).
[3] Y. Yamamoto and R. E. Slusher, Phys. Today **46**, 66 (1993).
[4] J. M. Gerard, B. Sermage, B. Gayral, B. Legrand, E. Costard, and V. Thierry-Mieg, Phys. Rev. Lett. **81**, 1110 (1998).
[5] S. Noda, A. Chutinan, and M. Imada, Nature (London) **407**, 608 (2000).
[6] E. Yablonovitch, Phys. Rev. Lett. **58**, 2059 (1987).
[7] S. John, Phys. Rev. Lett. **58**, 2486 (1987).
[8] T. F. Krauss, R. M. De La Rue, and S. Brand, Nature (London) **383**, 699 (1996).
[9] T. Baba, IEEE J. Sel. Top. Quantum Electron. **3**, 808 (1997).
[10] P. R. Villeneuve, S. H. Fan, J. D. Joannopoulos, K. Y. Lim, G. S. Petrich, L. A. Kolodziejski, and R. Reif, Appl. Phys. Lett. **67**, 167 (1995).
[11] J. Vučković, M. Lončar, H. Mabuchi, and A. Scherer, Phys. Rev. E **65**, 016608 (2002).
[12] H. Y. Ryu, S. H. Kim, H. G. Park, J. K. Hwang, Y. H. Lee, and J. S. Kim, Appl. Phys. Lett. **80**, 3883 (2002).
[13] J. M. Geremia, J. Williams, and H. Mabuchi, Phys. Rev. E **66**, 06606 (2002).
[14] O. J. Painter, R. K. Lee, A. Scherer, A. Yariv, J. D. O'Brien, P. D. Dapkus, and I. Kim, Science **284**, 1819 (1999).
[15] J. K. Hwang, H. Y. Ryu, D. S. Song, I. Y. Han, H. W. Song, H. K. Park, Y. H. Lee, and D. H. Jang, Appl. Phys. Lett. **76**, 2982 (2000).
[16] T. Yoshie, O. B. Shchekin, H. Chen, D. G. Deppe, and A. Scherer, Electron. Lett. **38**, 967 (2002).
[17] M. Lončar, T. Yoshie, A. Scherer, Y. Qiu, and P. Gogna, Appl. Phys. Lett. **81**, 2680 (2002).
[18] C. Monat, C. Seassal, X. Letartre, P. Viktorovitch, P. Regreny, M. Gendry, P. Rojo-Romeo, G. Hollinger, E. Jalaguier, S. Pocas, and B. Aspar, Electron. Lett. **37**, 764 (2002).
[19] P. T. Lee, J. R. Cao, S. J. Choi, Z. J. Wei, J. D. O'Brien, and P. D. Dapkus, Appl. Phys. Lett. **81**, 3311 (2002).
[20] T. D. Happ, M. Kamp, A. Forchel, J. L. Gentner, and L. Goldstein, Appl. Phys. Lett. **82**, 4 (2003).
[21] K. Srinivasan, P. E. Barclay, O. Painter, J. X. Chen, A. Y. Cho, and C. Gmachl, Appl. Phys. Lett. **83**, 1915 (2003).
[22] H. M. Gibbs, S. L. McCall, T. N. C. Venkatesan, A. C. Gossard, A. Passner, and W. Wiegmann, Appl. Phys. Lett. **35**, 451 (1979).
[23] K. Vahala, C. H. Harder, and A. Yariv, Appl. Phys. Lett. **42**, 211 (1983).
[24] C. R. Mirasso, G. H. M. van Tartwijk, E. Hernandez-Garcia, D. Lenstra, S. Lynch, P. Landais, P. Phelan, J. O'Gorman, M. San Miguel, and W. Elsasser, IEEE J. Quantum Electron. **35**, 764 (1999).
[25] Y. Yamamoto, S. Machida, and G. Bjork, Phys. Rev. A **44**, 657 (1991).
[26] P. A. Morton, T. Tanbunek T, R. A. Logan, N. Chand, K. W. Wecht, A. M. Sergent, and P. F. Scirtino, Electron. Lett. **30**, 2044 (1994).